High Energy Solar Physics: Anticipating HESSI
ASP Conference Series, Vol. xxx, 2000
R. Ramaty and N. Mandzhavidze, eds.

Millimeter–Interferometer Observations of Flares in Conjunction with HESSI

S. M. White & M. R. Kundu

Dept. of Astronomy, Univ. of Maryland, College Park MD 20742

Abstract. The nature of emission from solar flares at millimeter wavelengths is discussed. In the impulsive phase of flares, millimeter emission should be dominated by gyrosynchrotron emission from MeV–energy electrons. Millimeter telescopes are very sensitive to these electrons and can make high–resolution images of their sources for comparison with HESSI images, allowing us to investigate the behaviour of electron acceleration across a wide range of energies.

1. Introduction

The properties of MeV–energy electrons accelerated in solar flares are poorly understood. There is strong evidence (discussed below) that electrons of MeV energies have properties very different from those of lower energies which produce the bulk of the hard X–rays detected in flares. The implication is that they are not simply the high–energy extension of the nonthermal electron population carrying the bulk of the energy released in a flare, and that therefore a second acceleration mechanism may be required to explain the properties of these MeV–energy electrons. This would have important implications for our understanding of particle acceleration both in the solar atmosphere and elsewhere in astrophysics.

Detection of MeV–energy electrons via bremsstrahlung photons emitted at hard X–ray and γ–ray energies is a difficult task. Bremsstrahlung is increasingly inefficient as electron energy increases because faster electrons suffer less deflection by a nucleus. There is, however, another technique for detecting such energetic electrons which is much more sensitive than current hard X-ray detectors. Energetic electrons in coronal magnetic fields radiate strongly at millimeter wavelengths via synchrotron emission, and the synchrotron mechanism becomes more efficient as electron energy increases. This effect makes the use of a millimeter–wavelength radio interferometer a very powerful means for detecting such electrons. In this paper we discuss the nature of millimeter emission from solar flares and the prospects for observations of MeV–energy electrons with the BIMA interferometer as a complement to HESSI.

2. The BIMA Array

BIMA (Figure 1) is a synthesis array operating at millimeter wavelengths, and is the first such array to carry out extensive studies of solar emission. BIMA

Figure 1. The BIMA site, looking south down the lava–filled Hat Creek valley.

is operated by the universities of California at Berkeley (the PI institution for HESSI), Illinois and Maryland. BIMA is located in the Hat Creek valley of northern California, 5 hours north of San Francisco and about 3 hours from Reno. The telescope consists of 10 dishes operating in the 80-115 GHz range. BIMA has a 2 arcmin field of view and can image with arcsecond spatial resolution and time resolution of typically 2 seconds, and it has an excellent snapshot mapping ability. In addition to having the largest number of dishes of any of the world's millimeter arrays, BIMA also offers the longest baselines and therefore highest spatial resolution currently possible at 3 mm wavelength: down to $0''.3$.

3. Millimeter Emission from Solar Flares

Electrons moving in a magnetic field exhibit a gyration about the direction of the magnetic field, and the acceleration associated with this gyration leads to radiation by the gyromagnetic process. In the solar photosphere the magnetic field rarely exceeds 3000 G; in the corona it does not usually exceed 2000 G. Thus the gyrofrequency in the corona does not exceed $f_B = 2.8 \times 10^6\ B = 6$ GHz; more typically it is 2 GHz, and hence emission at 86 GHz (in the 3 mm atmospheric window) is typically around 40. Because the typical frequency of gyroemission of a particle with Lorentz factor γ is $\gamma^2 f_B$, nonrelativistic particles will not emit at such high harmonics; in particular, a thermal plasma, even at a temperature of 10^8 K, has negligible gyro–opacity at 86 GHz, and thus only nonthermal gyroemission by relativistic electrons can be seen at millimeter wavelengths. This is the basis for the argument that in solar flares the radio emission at millimeter

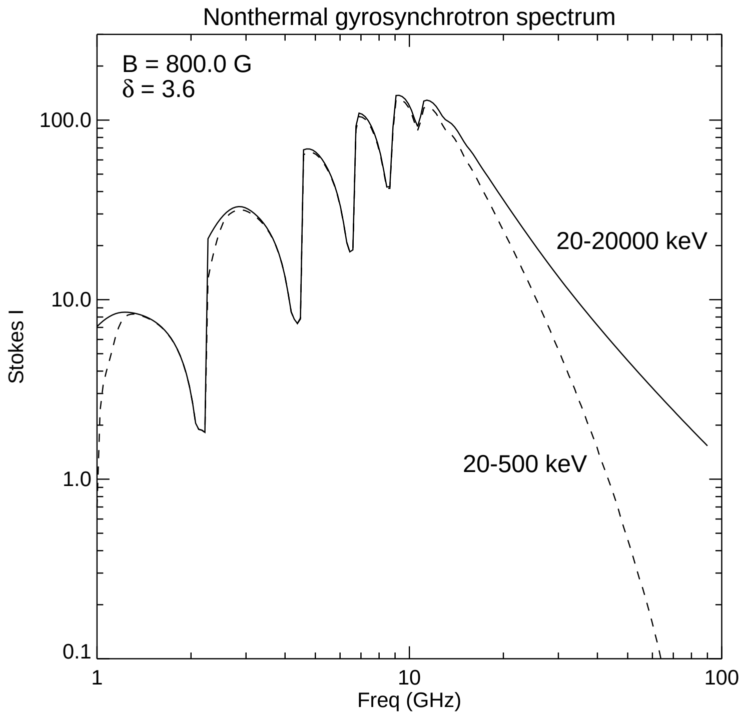

Figure 2. Figure showing the effect of MeV–energy electrons on the radio spectrum of the impulsive phase of a flare. The solid line shows the gyrosynchrotron spectrum emitted by electrons in a power-law distribution of energy spectral index −3.6 extending from 20 keV to 20 MeV in a constant magnetic field of 800 G. The dashed curve is the spectrum emitted by the same number of electrons in a power-law with the same energy spectral index but extending from 20 to 500 keV. When the MeV–energy electrons are absent, emission at millimeter wavelengths (e.g., the standard BIMA observing frequency of 86 GHz) is reduced by orders of magnitude.

wavelengths should be most sensitive to electrons with energies in excess of 1 MeV, i.e., those electrons whose bremsstrahlung should be in the gamma ray regime rather than those which emit hard X-rays in the range 25 – 100 keV. To quantify this statement, Figure 1 shows what happens to the gyrosynchrotron spectrum of radio emission from nonthermal electrons in a homogeneous magnetic field as one removes the higher energy electrons. When electrons up to 20 MeV are present the spectrum extends well into the millimeter range (the radio spectral index actually increases with frequency due to relativistic effects), but if electrons above 500 keV are removed, the high frequency spectrum (above the spectral peak at 10 GHz in this case) is strongly affected and increasingly so at higher frequencies. At our typical BIMA observing frequency of 86 GHz, removing electrons above 500 keV diminishes the observed flux by several orders of magnitude and such sources would not produce detectable nonthermal millimeter emission. Observations with a millimeter interferometer are very sensitive,

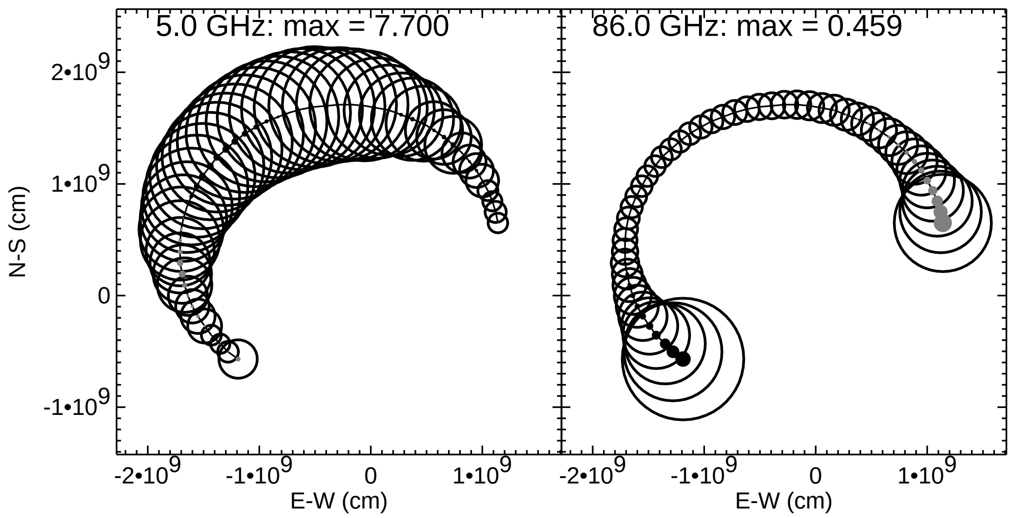

Figure 3. Model calculations of the radio emission from a flare loop filled with electrons at 5 GHz (upper) and 86 GHz (lower). The magnetic field in the loop varies by a factor of about 3 from looptop to footpoint. The energy spectral index of the electrons is 3.5 and the footpoint magnetic field is 800 G. Each open circle represents the total flux from a fixed length of loop, relative to the maximum value which is listed in each panel. Polarized fluxes are represented by filled circles which are either black or grey to represent the two senses of circular polarization. The loop is inclined at about 45° to the plane of the sky.

and can thus test whether or not "typical" solar flares produce MeV–energy electrons. The BIMA observations indicate that most small impulsive flares do indeed produce MeV–energy electrons (White et al. 1992; Kundu et al. 1994; White 1994; Silva et al. 1996, 1997; Raulin et al. 1999), and hence the required acceleration mechanism can operate even in conditions of relatively weak energy releases.

Figure 3 shows the appearance of a model flare loop at an optically thick microwave frequency (5 GHz) and an optically thin millimeter frequency (86 GHz). At the optically thick frequency the whole loop is bright, whereas at the higher frequency the strong magnetic field at the footpoints of the loop enhances the millimeter emission there and only the footpoints appear bright. In a loop filled with a population of trapped nonthermal electrons mirroring back and forth between the same magnetic field strength at both ends of the loop, we expect to see two footpoints at very high frequencies. In a loop where beaming produces significant precipitation at one footpoint but not the other, the images may show only one source. Thus the nature of the millimeter images can reveal a great deal about the nature of electron acceleration and propagation as well as the magnetic field geometry in the source.

Solar flares also produce much hot, dense plasma in the corona which emits strongly at soft X-ray wavelengths. This same plasma radiates strongly at millimeter wavelengths due to optically-thin thermal bremsstrahlung. However,

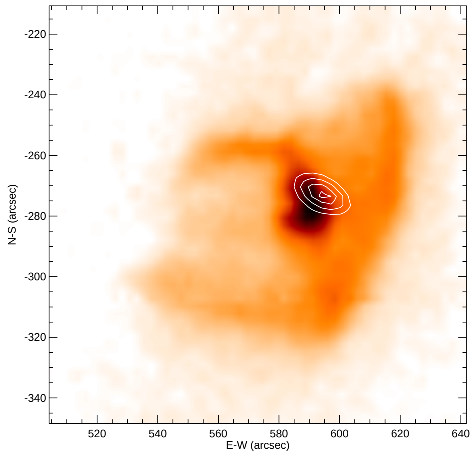

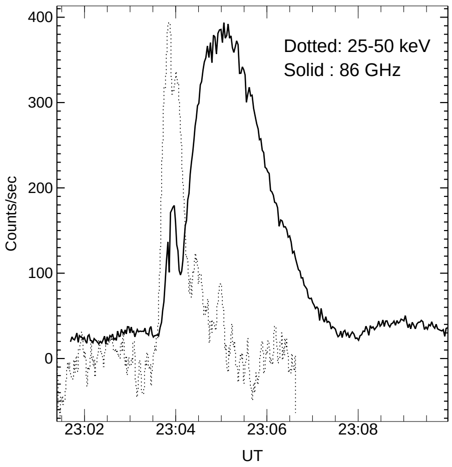

Figure 4. The left panel shows contours of the 86 GHz emission overlaid on a soft X–ray image of the post–flare loops in the solar corona. The location of the BIMA source is consistent with the northern footpoint of the soft X–ray loop. The right panel shows the time evolution of the event in hard X–rays (dashed histogram) and at 86 GHz (solid curve). Note that two components appear in the BIMA time profile, but only one of them shows associated nonthermal hard X–ray emission.

this emission is easily distingished from the nonthermal gyrosynchrotron emission by virtue of its timing and slowly–varying time profile: it is found always to be quite similar to the GOES soft X–ray time profile and is thus not a significant factor in the impulsive phase of most flares.

4. Millimeter Observations of Flares

BIMA observations have shown the remarkable result that MeV electrons are present in most flares, and even in events too small to be detected by GOES. More importantly, the MeV energy electrons can show properties quite different from those of the lower–energy electrons which dominate the hard X–ray emission, typically having a much flatter energy spectrum. Kundu et al. (this volume) present two well–observed examples of events which demonstrate the power of the high spatial resolution of which BIMA observations are capable. An event in which imaging data at millimeter wavelengths together with hard X–ray data allow much tighter constraints to be placed on the electron populations present is shown in Figure 4.

The time profile of the millimeter emission is compared (in the right panel) with the corresponding hard X–ray emission detected from this (small: GOES B6) event by GRO. Whereas the hard X–rays show only a single short–lived impulsive peak, BIMA shows two phases: a brief pulse of emission at the onset coincident with the hard X–rays, and then a second longer–duration component during which no X–rays are observed. The second component of the BIMA emission must also be due to nonthermal electrons since no other interpretation fits the data, yet they produced no hard X–rays: this may represent a population of electrons trapped in the corona where they can continue to radiate at millimeter wavelengths without producing any bremsstrahlung X–rays (Raulin et al. 1999). Data such as these provide important constraints for models of the spatial distribution of accelerated electrons in flares.

5. Prospects During the HESSI Mission

It is planned to request a BIMA campaign for the period in the northern summer immediately following the planned launch of HESSI in July 2000. This is a suitable time to request a substantial BIMA time allocation for solar work because summer daytime observations of weaker celestial sources are usually problematic. BIMA's field of view covers an entire active region. The array will be in a configuration containing both short and medium length baselines so that we can achieve a resolution of several arcseconds while simultaneously being sensitive to large sources (such as two footpoints $40''$ apart). Assuming solar activity levels characteristic of solar maximum, we could detect an average of 2 flares per day resulting in a database of 50–100 events, with up to half of these having simultaneous HESSI data. Flare event data will be calibrated and mapped and we will then make quick–look image cubes available via a web–accessible archive in a format (FITS) suitable for further analysis in IDL and compatible with SolarSoft standards. More detailed analysis of individual events can then be carried out in collaboration with outside observers interested in particular events.

Solar radio research at the University of Maryland is supported by NSF grants ATM 96-12738 and INT 98–19917 and NASA grants NAG 5-7370, NAG 5-6257 and NAG 5-7901. The use of BIMA for scientific research at the University of Maryland is supported by NSF grant AST 93–14847.

References

Kundu, M. R., White, S. M., Gopalswamy, N., & Lim, J. 1994, ApJS, 90, 599

Kundu, M. R., White, S. M., Shibasaki, K. & Sakurai, T. 2000, in the proceedings of the High Energy Solar Physics Workshop: Anticipating HESSI, ed. R. Ramaty & N. Mandzhavidze (San Francisco: ASP), in press

Raulin, J., White, S. M., Kundu, M. R., Silva, A. R., & Shibasaki, K. 1999, ApJ, 522, 547

Silva, A. V. L., White, S. M., Lin, R. P., de Pater, I., Shibasaki, K., Hudson, H. S., & Kundu, M. R. 1996, ApJL, 458, L49

Silva, A. V. L., Gary, D. E., White, S. M., Lin, R. P., & de Pater, I. 1997, Solar Phys., 175, 157

White, S. M., Kundu, M. R., Bastian, T. S., Gary, D. E., Hurford, G. J., Kucera, T., & Bieging, J. 1992, ApJ, 384, 656

White, S. M. 1994, in High Energy Solar Phenomena: A New Era of Spacecraft Measurements, ed. J. Ryan & W. T. Vestrand (New York: American Institute of Physics (Conf. Proc. **294**)), p. 199.